Dewetting of Thin Diblock Copolymer Films: Spinodal Dewetting Kinetics

P. Müller-Buschbaum,*,† J. S. Gutmann,‡,|| C. Lorenz-Haas,§ O. Wunnicke,‡ M. Stamm,‡ and W. Petry†

Physik-Department, LS E13, TU München, James-Franck-Str.1, 85747 Garching, Germany; Institut für Polymerforschung Dresden e.V., Hohe Str. 6, 01069 Dresden, Germany; and Max-Planck-Institut für Polymerforschung, Ackermannweg 10, 55128 Mainz, Germany

Received February 1, 2001; Revised Manuscript Received October 23, 2001

ABSTRACT: The stability of thin diblock copolymer films with respect to the annealing above the microphase separation temperature is investigated on long time scales and at different film thicknesses. Poly(styrene-*block*-*p*-methylstyrene) diblock copolymer films on top of silicon substrates are examined with scanning force microscopy and off-specular X-ray scattering. At film thickness below the lamellar spacing of the bulk material a dewetting is observed. The kinetics of the film destabilization are explainable within a spinodal dewetting model. The observed dewetting structures belong to a wet dewetting. In the case of film thicknesses which enable the buildup of a few lamellae no sign of instability was detected.

Introduction

Diblock copolymers exhibit various technological important applications which result from their special chemical structure. Because of the chemical linkage of two immiscible polymers A and B, a macrophase separation is prevented. Phase separation leads to pattern formation on nanometer length scales.[1] To reduce the number of energetically unfavorable interactions between distinct blocks, the molecules organize into complex morphologies. The morphology is selected by minimizing the free energy for the buildup of internal interfaces compared to the conformational entropy to adopt this morphology.[2−5] For symmetric diblock copolymers, in which both blocks occupy equal volume fractions, a lamellar orientation is preferred. By varying the relative volume fractions, spherical, cylindrical, bicontinuous, or more complex morphologies can be formed.[6,7] A variation of the chemical block composition affects the properties of the domains. In contrast to bulk samples, in thin films the interactions with both boundaries influence the morphology as well as its orientation. In the case of complete wetting of each interface by one component of the diblock copolymer, a lamellar order parallel to the interfaces is forced.[8−13] If one interface is free, like a film surface toward vacuum, the film thickness is quantized in units of the lamellar bulk period L. If the initial film thickness is not commensurate with this constraint, an incomplete top layer is formed.[14] This commensurability effect basically affects the morphology of the surface, and islands or holes are created.[15,16] With decreasing film thickness the confinement gives rise to an interplay between the intrinsic length scale of the bulk structure and the geometry of the film.[17−20] This leads to transitions between phases of identical symmetry but different orientation with respect to the confining walls. As an example lamellar domains reorient from a parallel to a perpendicular arrangement.[21]

Usually samples are annealed to adopt the equilibrium morphology. Despite morphologies originated by commensurability effects, surface morphologies due to the dewetting of a diblock copolymer film are only rarely reported.[22] Thin diblock copolymer films show basically no tendency toward destabilization.[23,24] In contrast, the destabilization of thin films on top of solid substrates was largely observed in the case of homopolymer or polymer blend systems.[25−35] The internal lamellar order prevents thin diblock copolymer films from dewetting in many sample systems. Even a perpendicularly aligned lamellae was reported to stay stable during extremely long annealing in the case of poly(styrene-*block*-methyl methacrylate) samples.[21] In the present investigation we focus on a possible destabilization of diblock copolymer films in more detail. The model system chosen is poly(styrene-*block*-*p*-methylstyrene), denoted P(S-*b*-pMS), which is characterized by the weak incompatibility of both components polystyrene (PS) and poly(*p*-methylstyrene) (PpMS)[36−38] and the strong surface segregation of the PpMS component.[39,40] Consequently, a lamellar order is already installed right after preparation. Its periodicity is different as compared to the equilibrium bulk state, and it rearranges during annealing.[41,42] In the case of very thin films the PpMS component likes to wet both interfaces.

The article is structured as follows: The introduction is followed by an Experimental Section describing the sample preparation and the techniques used. The sections on results and discussion are followed by a summary and an outlook.

Experimental Section

Sample Preparation. For our experiments we used a symmetric poly(styrene-*block*-*p*-methylstyrene) diblock copolymer, denoted P(S-*b*-pMS), with a molecular weight M_w = 230 000 g/mol, a polydispersity $M_w/M_n = 1.08$, and a styrene fraction of the copolymer of $f_{PS} = N_{PS}/N = 0.47$. The diblock copolymer material was prepared anionically and was obtained from Polymer Standard Service, Mainz. To prepare thin films,

† TU München.
‡ Institut für Polymerforschung Dresden e.V.
§ Max-Planck-Institut für Polymerforschung.
|| Present address: Department of Materials Science and Engineering, 330 Bard Hall, Cornell University, Ithaca, New York.
* Corresponding author.

10.1021/ma010192y CCC: $22.00
Published on Web 02/07/2002

a toluene solution was spin-coated (1950 rpm for 30 s) on top of native oxide-covered Si(100) surfaces (MEMC Electronic Materials Inc., Spartanburg). Prior to the spin-coating, the substrates were cleaned in an acid bath. The cleaning bath consists of 100 mL of 80% H_2SO_4, 35 mL of H_2O_2, and 15 mL of deionized water. After 15 min at 80 °C in the acid bath the substrates were taken out, rinsed in deionized water, and dried with compressed nitrogen. Immediately before coating the dry substrates were flushed with fresh toluene. Several samples were prepared out of the same solution. The annealing of the samples was performed in a vacuum furnace at $T = 161.8$ °C. This temperature is well above the microphase separation temperature $T_{MST} = 153 \pm 4$ °C.[39,42,43] Thus, the copolymer is annealed in its disordered state. After the chosen annealing time the samples were quenched down to room temperature, which is well below the glass transition temperature of both copolymers, and examined. To check the reproducibility of the reported results, several samples were prepared and investigated.

Scanning Force Microscopy. A PARK Autoprobe CP atomic force microscope (SFM) is used for the investigation of the diblock copolymer film surfaces. We used silicon gold-coated conical cantilevers, with a spring constant of ≅2.1 N m^{-1} and a high aspect ratio. The tip has a typical radius of curvature of 100 Å. The image acquisition was done in air at room temperature. To minimize tip-induced sample degradation, all measurements were performed in noncontact mode. Several images were measured for each sample. Micrographs were recorded at different sample positions using scan ranges between 5 μm × 5 μm and 80 μm × 80 μm. From the raw data the background due to the scanner tube movement is fully subtracted to determine the values of the rms roughness over the complete scan area. The rms roughness values were calculated for each individual scan range. In addition to this statistical information perpendicular to the sample surface, statistical information parallel to the surface is obtained from the power spectral density function (PSD).[44,45] The PSD is calculated from the SFM height data by a 2D Fourier transformation and radially averaging of the isotropic Fourier space data. Because of the different scan ranges in real space, the PSD cover different intervals in reciprocal space. Thus, a combination of PSD related to different scan ranges enlarges the covered interval in reciprocal space as compared to one individual PSD. In the following the combined PSD data is called master curve. It is equivalent to a scattering signal and thus pictures the existence of a most prominent in-plane length scale which might be present within the resolvable range. If a distinct peak is present in the master curve, the most prominent in-plane length Λ is extracted from its position. With the rms roughness and the master curve the sample surface is described in a statistical sense.

X-ray Specular Scattering. With a laboratory X-ray source ($\Theta-\Theta$ reflectometer Seifert XRD 3003TT) reflectivity measurements of the samples were performed. A Ge(110) channel cut crystal is used to monochromasize the beam (λ = 1.54 Å). The sample is placed on a special designed vacuum chuck and is measured under air. Reflectivity curves of the as-prepared films exhibit well-pronounced fringes due to the small surface roughness of typically 5 Å. From a fit to the reflectivity data the film thicknesses of the as-prepared samples l were obtained.[46−48] The density resembles the mean density of both components PS and PpMS. Because of the weak scattering contrast, a resolution of the internal order is quite difficult.[49]

X-ray Off-Specular Scattering. At the synchrotron HASYLAB (DESY, Hamburg) at the BW4 beamline the diffuse scattering was measured. For further details concerning the beamline see ref 50. The sample was placed horizontally on a two-circle goniometer with a z-translation table. We used a setup of high-quality entrance slits and a completely evacuated pathway. At the selected wavelength $\lambda = 1.38$ Å due to the sample−detector distance of 2.87 m with the two-dimensional detector consisting of a 512 × 512 pixel array one detector scan and several off-detector scans were measured together. At a fixed incident angle of $\alpha_i = 1.02°$ the prominent features in a detector scan, the specular as well as the Yoneda peak,[51,52] are well-separated. A schematic picture of this scattering geometry is shown in Figure 1.

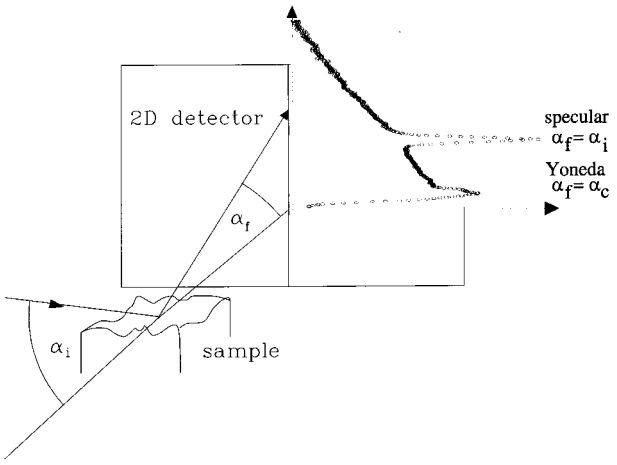

Figure 1. Schematic picture of the experimental setup used at the BW4 beamline. The incident angle onto the horizontally placed sample surface is denoted α_i and the exit angle α_f. A two-dimensional detector is used to measure one complete set of a detector and several off-detector scans. As figuratively shown, the diffusely scattered intensity in the scattering plane, the detector scan, exhibits a Yoneda peak and a specular peak as common features.

Results and Discussion

Spinodal Dewetting Model. Within the spinodal dewetting model[25] a thermally induced thickness modulation created at the interface can be approximated by an expression $z(x,t) = l + \delta l \exp(iqx)$. The oscillatory amplitude of the surface fluctuations $\delta l = \delta l_0 \exp(t/\tau)$ has a wavelength $\Lambda = 2\pi/q$. The coordinate parallel to the surface is denoted with x, the homogeneous film thickness with l, the wave vector with q, and the relaxation time with τ. In the linearized model the initial fluctuations are amplified exponentially with the fastest growing wave vector $q_m = \sqrt{(3/2)}(a/l^2)$ and a relaxation time of the instability $\tau_m = \pi\eta l^5/(6a^2)$ where η is the viscosity, γ the surface tension, and a a molecular length which depends on the van der Waals interaction.[25]

Thin Film. We choose a film thickness of $l = 300$ Å as determined with X-ray reflectivity right after preparation. Therefore, the films are thin as compared to the bulk lamellar period $L = 450$ Å,[38−41] which corresponds to the thickness of an ABBA or BAAB bilayer. With small-angle neutron scattering experiments a radius of gyration of $R_g = 136$ Å[42,43] was determined. Because of the film thickness l still being larger than twice this radius of gyration $2R_g$, confinement effects should not be dominant. In general, PpMS prefers to segregate at the film surface due to the large differences in the surface energies of both components PS and PpMS (γ(PpMS)/γ(PS) = 0.86). Whereas in thick films the lamellar order induced by this surface segregation decays toward the bulk, in thin films the ratio of film thickness l and lamellar spacing L becomes important.[39−41] In the model system P(S-*b*-pMS) the lamellar order is installed right after preparation as well as after annealing.[10,41] However, the initial periodicity $\tilde{L} = 240 \pm 10$ Å, which commonly installs right after preparation in the case of thick P(S-*b*-pMS) films,[10,41] is smaller than the bulk lamellar period L. In the case of 300 Å film

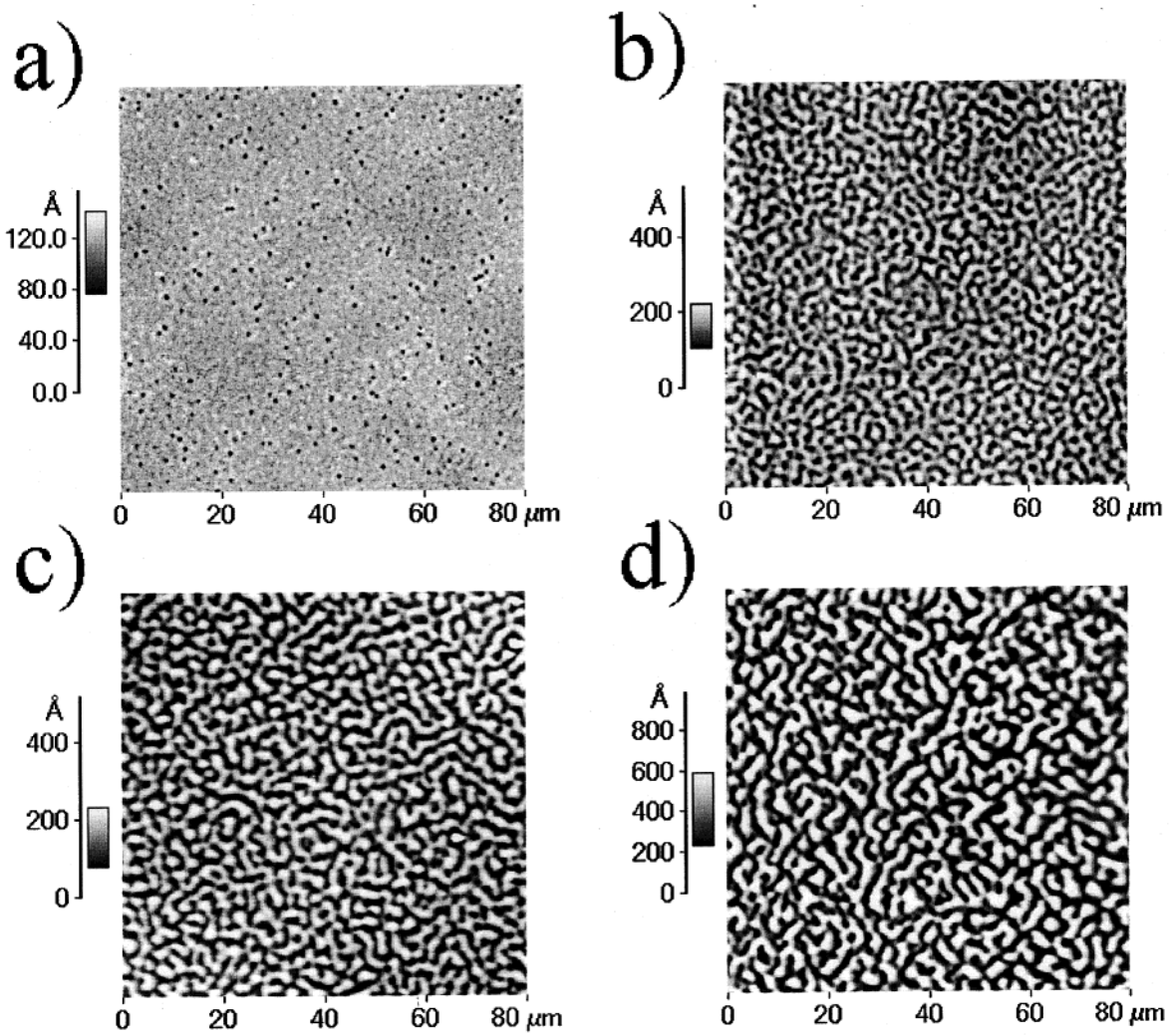

Figure 2. SFM pictures (scan range 80 × 80 μm^2) of the topology signal as observed after annealing: (a) 284.5, (b) 400, (c) 725.5, and (d) 1874 h. The height scaling is different for each pattern to show the in-plane structure more clearly.

thickness the surface tension force a surface segregation of PpMS, but the limited available volume of polymeric material ($l = 6\tilde{L}/5 = 2L/3$) prevents the buildup of a complete lamella. As determined with ^{15}N nuclear reaction analysis in previous investigations[40] right after preparation, the PpMS block segregates to the surface and the laterally averaged PpMS contend decays monotonically without any further internal ordering. After annealing, a buildup of a bulk lamellar order is suppressed as well,[40] and the PpMS enrichment at the surface is conserved. The formation of islands is energetically forbidden due to the big difference in the surface energies of both components PS and PpMS. As determined with specular and off-specular scattering as well as with SFM, the diblock copolymer film stays homogeneous during annealing above the microphase separation temperature[53] for many hours. Consequently, right after preparation as well as after annealing a surface segregation of the PpMS component results, and the volume fraction of PpMS decays toward the silicon substrate surface. In terms of the PS component its volume fraction is enriched at the substrate surface. Nevertheless, in this special film thickness range the diblock copolymer film is frustrated. For energetic reasons the PpMS block would prefer both boundaries. This gives rise to a further mechanism for the minimization of the excess free energy density, the dewetting of the complete film. In the literature the dewetting of diblock copolymer films is rarely reported.[22,54,55]

In Figure 2 we present four examples of the successively evolving surface morphologies as measured with SFM during the annealing at $T = 161.8$ °C. Thus, the samples are annealed in the disordered state. A large scan range of 80 μm × 80 μm is chosen to give an impression of the uniformity of the morphologies. After 284.5 h annealing small holes are visible first (Figure 2a). The holes are surrounded by small rims which include the excess material. These holes grow in lateral size as well as in depth, and after 400 h the surface has clearly roughened further (Figure 2b); the resulting morphology resembles a bicontinuous spinodal-like pattern. After 725.5 h (Figure 2c) and 1874 h (Figure 2d) the surface has coarsened further without changing the morphology type. After 4157 h still no drop morphology is created, which underlines the small velocity of this dewetting process. A comparably thick homopolymer film of polystyrene (PS) or poly(*p*-methylstyrene) (PpMS), if unstable on the corresponding surface, dewetted within a fraction of this time.

Typical line scans of the SFM data are presented in Figure 3. From the bottom to the top data from samples annealed for 24, 284.5, 400, 484, 725.5, and 1874 h are shown. Note that the scaling of the *x*-axis, displaying the lateral sample position, and the *z*-axis, displaying

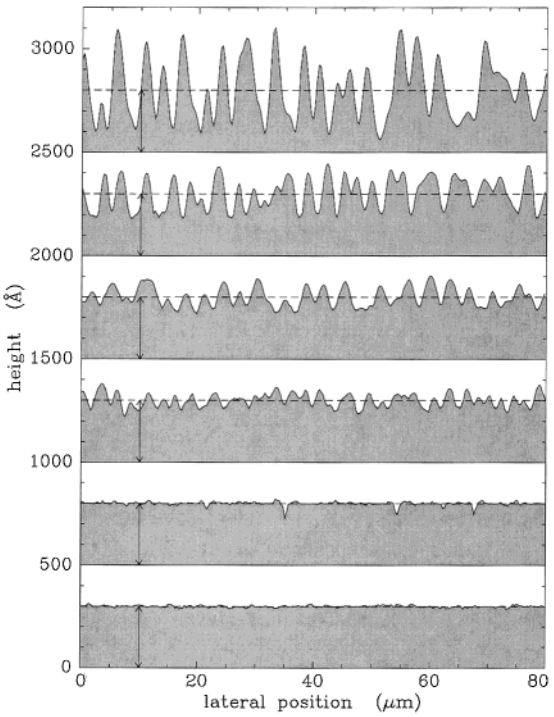

Figure 3. Line scans from SFM data measured after different annealing times. From the bottom to the top the samples were annealed for 24, 284.5, 400, 484, 725.5, and 1874 h. The film volume is printed in gray. The mean film thickness is shown with the dashed line. Data are shifted for clarity.

the height, are different by a factor of ≅250 to emphasize on the surface topology. In addition, the line scans are shifted by 500 Å against each other along the *z*-axis to enable a picturing of the evolving structures with increasing annealing time from the bottom to the top. The mean surface height as determined with X-ray reflectivity is visualized with the dashed lines, and the film volume is plotted in gray. After a short annealing like 24 h the film is homogeneous and basically smooth with an rms surface roughness σ_{rms} on the order of 5 Å. This is in good agreement with previous observations that showed that annealed diblock copolymer films of P(S-*b*-pMS) are essentially homogeneous after annealing.[10,39−41,53] First holes are present after 284.5 h annealing, which is clearly much longer as compared to previous annealing experiments. Thus, the creation of these first holes which do not rupture down to the substrate surface was not observed until now. Because of the extremely slow process, the line scans shown in Figure 3 exhibit the early stages of the diblock copolymer film dewetting. Although the peak to valley amplitude of the surface roughness as well as its lateral wavelength increases, a dewetting down to the substrate needs more than 4157 h of annealing at $T = 161.8$ °C. Of course, an increase of the annealing temperature would speed up the process and thus shrink the experimentally required time window. Nevertheless, even at a drastically higher annealing temperature like $T = 195$ °C it took more than 208 h. This gives a first hint that the observed dewetting is not driven by a nucleation and growth process. Commonly nucleated dewetting is much faster as compared to a spinodal process. However, the film does not rupture into droplets until the total height variation becomes equal to the total film thickness. This is consistent with the general rupture criterion for the breakup of liquid or homopolymer films.[56]

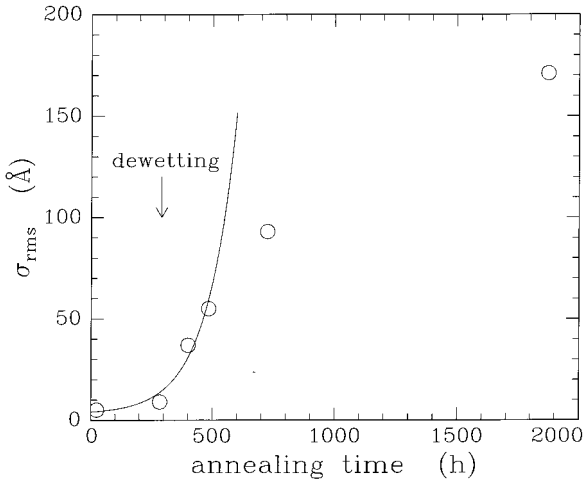

Figure 4. Rms surface roughness σ_{rms} plotted as a function of the annealing time *t*. The symbol size pictures the error bar of the experimental data. The solid line is a model fit based on an exponential growth model.

To obtain a less pictorial but more statistical description, the rms surface roughness was calculated from the SFM data. From the X-ray reflectivity data only the values at shorter annealing times are yielded, due to the drastic increase in surface roughness. Figure 4 shows the surface roughness σ_{rms} as a function of annealing time *t*. After ≅300 h the surface roughness starts to increase significantly. For the initial stages of the dewetting the experimental data show a nonlinear growth. The solid line in Figure 4 follows $\sigma_{rms} \sim \exp(t)$ in accordance with the predictions of the spinodal dewetting model.[57,58] A slowing down of the exponential growth occurs when the total average height variation approaches half the film thickness as observed previously in homopolymer films as well.[33] However, because of the limited number of data points, other nonlinear growth models cannot be excluded.

Besides the time evolution of the amplitude of the surface roughness, the spinodal dewetting model predicts the scale of the in-plane surface undulations. During the early stages of the dewetting process, the characteristic wave vector q^* corresponds to the size of the most stable surface undulations.[25,57] From the master curve calculated from the SFM data the most prominent in-plane length scale Λ is obtained by a determination of the peak position $q_m = 2\pi/\Lambda$. In Figure 5 two master curves corresponding to different annealing times are shown. The position of $q_m = q^*$ shifts toward smaller wave vectors q with increasing annealing time. It is then possible to define a crossover wave vector q_c, such that thickness fluctuations grow in amplitude for $q < q_c$, while those with $q > q_c$ decay with time. Relative intensity data at other annealing times in the early stages of the dewetting (not shown for clarity) also cross at q_c. The ratio of the both inverse lengths as shown in Figure 5 is $q_c/q_m = 1.38$. This value is in good agreement with the theoretically predicted one $q_c/q_m = \sqrt{2} = 1.41$, which gives the next correspondence between the spinodal dewetting model and the experimental data. A similar observation was up to now only reported in homopolymer films,[33] but not in diblock copolymer films.

A double-logarithmic plot of the most prominent in-plane length Λ as a function of the annealing time *t* suggests two distinct stages of the spinodal dewetting

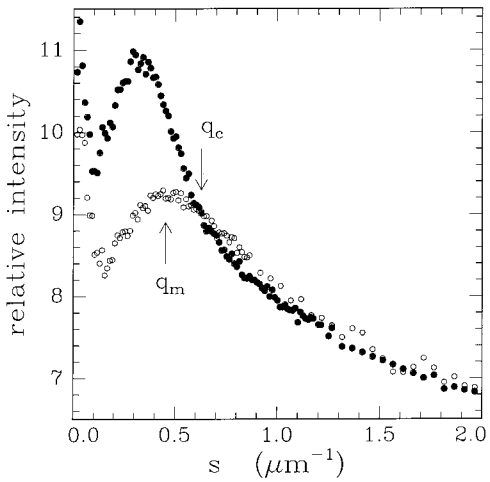

Figure 5. Comparison of the relative intensities of the master curves calculated from the SFM data after 284.5 h (open circles) and 484 h (solid circles) of annealing. The data are plotted as a function of the inverse length $s = q/2\pi$. The peak position q_m as well as the crossover wave vector q_c is marked.

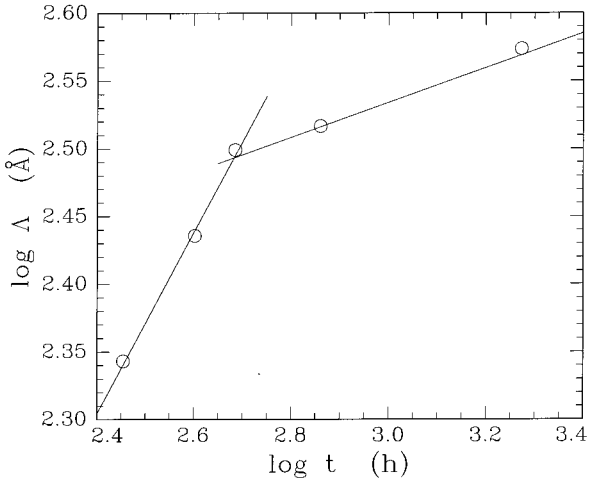

Figure 6. Double-logarithmic plot of the most prominent in-plane length Λ as a function of the annealing time *t*. The solid lines have slopes of $^2/_3$ for the short annealing times and $^1/_3$ for the long annealing times.

process (see Figure 6). In the early stage the data agree well with a $\Lambda \sim t^{2/3}$ behavior, whereas for the late annealing stages a $\Lambda \sim t^{1/3}$ behavior is observed. Theoretically, the kinetics of film destabilization depend on the viscosities of both materials, the substrate η_s and the polymer layer η_l.[59] With Θ denoting the contact angle between the film and the substrate, the ratio of $\eta_s/(\eta_l/\Theta)$ determines whether in-plane length scales increase with $\Lambda \sim t$ ($\eta_s > \eta_l/\Theta$) or with $\Lambda \sim t^{2/3}$ ($\eta_s < \eta_l/\Theta$). In the case of a dewetting on top of itself both viscosities are equal, and because of the small contact angles (measured value $\Theta = 0.3°$), the condition $\eta_s < \eta_l/\Theta$ is fulfilled. Consequently, our experimental data are in good agreement with the wet dewetting case,[60] which fits well to the fact that during this early stage the holes do not reach the substrate (see Figure 3). The situation changes again during the late stages. Obviously, in the case of roughness amplitudes which are on the order of half of the film thickness the kinetics slow down. One has to keep in mind that in the presented investigation we focus on diblock copolymers, which thus have an internal chemical structure, which

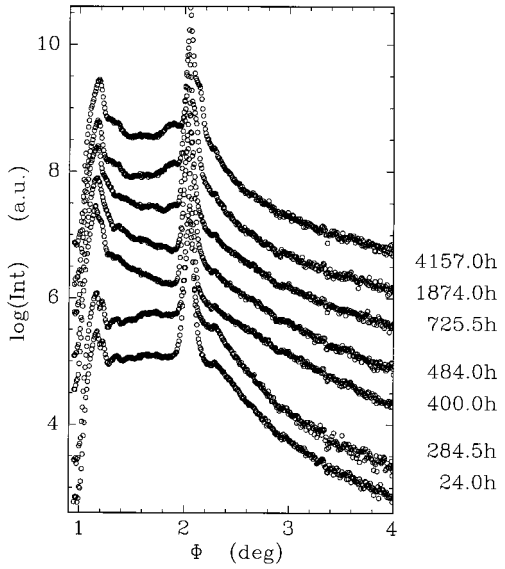

Figure 7. Detector scans measured at the angle of incidence $\alpha_i = 1.01°$ of films annealed ex-situ at $T = 161.8$ °C for different times. For clarity, the curves are shifted by $^1/_2$ order of magnitude against each other.

decreases the molecule mobility. On the other hand, both components PS and PpMS are only weakly incompatible,[42,43] and PpMS has a strong preference for surface segregation.

In addition to the real space analysis with SFM the samples are investigated with off-specular X-ray scattering. Performing detector scans the correlation perpendicular to the sample surface, which is not accessible with SFM, is analyzed. In a detector scan the sample is held fixed at one angle of incidence α_i, and the detector position is varied. Figure 7 shows these detector scans for different annealing times between 24 and 4157 h. The intensity is plotted on a logarithmic scale as a function of the detector angle $\Phi = \alpha_i + \alpha_f$. In horizontal direction the intensity was integrated over $\Delta q_y = \pm 3.12 \times 10^{-3}$ Å^{-1}. Marked features are the Yoneda peak which is observed at $\Phi_y = 1.19°$ and the specular peak visible at $\Phi_s = 2.04°$. The Yoneda peak is generated by an enhancement of the transmitted wave amplitude at the inner sample surface.[51,52]

Scans measured after 24 and 284.5 h are nearly equal in shape, which proves that the presence of the first holes on the film surface, as observed with SFM, does not affect the internal film structure. As measured with ^{15}N nuclear reaction analysis,[40] PpMS is enriched at the surface. The Yoneda peak is split up into two well-separated peaks at the positions corresponding to the critical angle of the diblock copolymer P(S-*b*-pMS) and of the Si substrate. Both peaks are nearly equal in their intensity, due to a very similar surface roughness of the polymer surface and the substrate surface. After 400 h annealing the scattering curve has significantly changed. The changes are present in the shape of the Yoneda peak as well as in the detector angle dependence of the intensity decay. The intensity of the Yoneda peak at smaller angles, belonging to the diblock copolymer film increases as compared to the one belonging to the Si substrate. This pictures the roughening of the polymer surface, whereas the substrate surface is not affected by the annealing. After 484 h of annealing the Yoneda contribution of the Si substrate has vanished basically due to the increased roughness of the polymer surface.

In addition slight modulations of the intensity between the Yoneda peak and the specular peak are observable. During further annealing these modulations are shifting in their wavelength and increase in their amplitude. In general, modulations in a detector scan can be originated by resonant diffuse scattering or by a dynamic scattering effect. Both are special types of diffuse scattering and thus related with the in-plane morphology in terms of a local film information. Resonant diffuse scattering is caused by roughness correlation between the film surface and the substrate surface. Because of the dominant surface features as visualized with SFM, a correlation between the polymer film surface and the silicon substrate surface can be excluded. Consequently, the modulations result from the dynamic effect.[52] The interference fringes are created due to a waveguide behavior of the two interfaces in the layer structure: the substrate−homogeneous film interface and the homogeneous−dewetted film interface. The Yoneda wing can be understood as the zero-order resonance. Higher orders $m_{i,f}$ of these dynamically originated fringes are damped out toward larger q_z values. They occur independent of the actual interface correlation function if the modified Bragg condition $2d^{dyn}\sqrt{n^2-\cos^2(\alpha_{i,f})} = m_{i,f}\lambda$ is fulfilled. Thus, from the wavelength of the modulation Δq_z the distance d^{dyn} of the interfaces causing this dynamic effect is calculated using $\Delta q_z = \pi/d^{dyn}$. From the X-ray data values of d^{dyn} = 265 Å (400 h), 186 Å (484 h), 154 Å (725.5 h), and 100 Å (1874 and 4157 h) were extracted. These values agree quite well with the values of the homogeneous film remaining on the substrate d^{homog} obtainable from the SFM data (d^{homog} = 250, 220, 180, 100, and 80 Å). But in contrast to the very local information on any SFM measurement, the diffuse X-ray scattering statistically averages over the sample structures. In agreement with the SFM information, the scattering information displays the dewetting of the diblock copolymer film on top of itself.

Thick Film. For a comparison a larger film thickness of l = 1190 Å was examined as well. The film thickness was again determined with X-ray reflectivity right after preparation. As compared to the bulk lamellar period L = 450 Å,[38−41] this corresponds to nearly three lamellae ($l = 11L/4$). During the annealing within 4157 h no sign of dewetting, like first holes, or a significant roughening of the diblock copolymer film surface was observable with SFM or X-ray scattering. On one hand, we might attribute this to the stabilization of the film due to internal creation of lamellae which satisfy the boundary conditions of an PpMS enrichment at both interfaces. On the other hand, because of the strong influence of the film thickness on the characteristic rupture time $\tau \sim l^5$ within the spinodal dewetting model,[57] a film thickness increase of nearly 4 times shifts the onset of the dewetting by a factor of 1000. Thus, on the time scale of the experiment this film remains stable. However, the stability of thicker P(S-*b*-pMS) films is in good agreement with previous experimental observations.[10,39−41]

Summary and Outlook

We present experimental results that strongly suggest that thin diblock copolymer P(S-*b*-pMS) films dewet via a spinodal dewetting process. As common in every dewetting investigation, the severe cleaning of the substrate is important to avoid a nucleated dewetting. A quite long annealing time of the diblock copolymer film in its isotropic phase is required to rupture the homogeneous film by introducing first holes in the film. As predicted by the spinodal model, the amplitude of the surface roughness increases nonlinear with time and the ratio of the characteristic and the crossover wave vector obeys the predicted law. The observed time dependence of the lateral length scales implies a wet dewetting. The presence of a homogeneous underlying polymer layer which decreases in its thickness with time is proven by the X-ray scattering experiment as well. As compared to homopolymer films, the kinetics are generally slowed down, which might be a result of the chemical structure of the diblock copolymer molecule. At larger film thickness no sign of dewetting was detected within the experimental time window, which again is in agreement with a spinodal dewetting model. Annealing experiments on time scales longer than half a year do not seem reasonable to the authors, and films might be called practically stable, if homogeneous after this annealing time. With future experiments one might address even smaller film thicknesses. At a further decreased film thickness confinement effects will be no longer negligible. This might introduce additional aspects in the dewetting process and is beyond the scope of this investigation.

Acknowledgment. We thank S. Cunis and G. von Krosigk for their help at the BW4 beamline at the HASYLAB. Additionally, we owe many thanks to R. Gehrke for his general support of the experiment at HASYLAB. This work was supported by the BMBF (Förderkennzeichen 03DUOTU1/4). C.L-.H. was supported by Graduiertenkolleg "Physik und Chemie Supramolekularer Systeme" Mainz University and O.W. by the DFG Schwerpunktprogramm "Benetzung und Strukturbildung an Grenzflächen" (Sta 324/8-2).

References and Notes

(1) Hamley, I. W. *The Physics of Block Copolymers*, Oxford University Press: New York, 1998.
(2) Fredrickson, G. H. *Macromolecules* **1987**, *20*, 2535.
(3) Turner, M. S. *Phys. Rev. Lett.* **1992**, *69*, 1788.
(4) Fischer, M. E.; Nakanishi, H. *J. Chem. Phys.* **1981**, *75*, 5857.
(5) Tang, W. H. *Macromolecules* **2000**, *33*, 1370.
(6) Bates, F. S.; Fredrickson, G. H. *Annu. Rev. Phys. Chem.* **1990**, *41*, 515.
(7) Alexandridis, P.; Spontak, R. J. *Curr. Opin. Colloid Interface Sci.* **1999**, *4*, 130.
(8) Anastasiadis, S. H.; Russell, T. P.; Satija, S. K.; Majkrzak, C. F. *Phys. Rev. Lett.* **1989**, *62*, 1852.
(9) Russell, T. P.; Coulon, G.; Deline, V. R.; Miller, D. C. *Macromolecules* **1989**, *22*, 4600.
(10) Stamm, M.; Götzelmann, A.; Giessler, K.-H.; Rauch, F. *Prog. Colloid Polym. Sci.* **1993**, *91*, 101.
(11) Mansky, P.; Russell, T. P.; Hawker, C. J.; Mays, J.; Cook, D. C.; Satija, S. K. *Phys. Rev. Lett.* **1997**, *79*, 237.
(12) Torikai, N.; Noda, I.; Karim, A.; Satija, S. K.; Han, C. C.; Matsushita, Y.; Kawakatsu, T. *Macromolecules* **1997**, *30*, 2907.
(13) Vignaud, G.; Gibaud, A.; Grübel, G.; Joly, S.; Ausserre, D.; Legrand, J. F.; Gallot, Y. *Physica B* **1998**, *248*, 250.
(14) Mansky, P.; Russell, T. P.; Hawker, C. J.; Pitsikalis, M.; Mays, J. *Macromolecules* **1997**, *30*, 6810.
(15) Stocker, W.; Beckmann, J.; Stadler, R.; Rabe, J. P. *Macromolecules* **1996**, *29*, 7502.
(16) Huang, E.; Mansky, P.; Russell, T. P.; Harrison, C.; Chaikin, P. M.; Register, R. A.; Hawker, C. J.; Mays, J. *Macromolecules* **2000**, *33*, 80.
(17) Turner, M. S. *Phys. Rev. Lett.* **1992**, *69*, 1788.
(18) Geisinger, T.; Müller, M.; Binder, K. *J. Chem. Phys.* **1999**, *111*, 5241.
(19) Geisinger, T.; Müller, M.; Binder, K. *J. Chem. Phys.* **1999**, *111*, 5251.

(20) Tang, W. H. *Macromolecules* **2000**, *33*, 1370.
(21) Morkved, T. L.; Jaeger, H. M. *Europhys. Lett.* **1997**, *40*, 643.
(22) Hamley, I. W.; Hiscutt, E. L.; Yang, Y. W.; Booth, C. *J. Colloid Interface Sci.* **1999**, *209*, 255.
(23) Dietrich, S. In *Phase Transitions and Critical Phenomena*; Domb, C., Lebowitz, J. L., Eds.; Academic: New York, 1988; Vol. 12.
(24) Israelachvili, J. N. In *Intermolecular and Surface Forces*, 2nd ed.; Academic Press: London, 1991.
(25) Brochard-Wyart, F.; Redon, C.; Sykes, C. *C. R. Acad. Sci., Ser.2* **1992**, *19*, 314.
(26) Reiter, G. *Phys. Rev. Lett.* **1992**, *68*, 75.
(27) Reiter, G. *Langmuir* **1993**, *9*, 1344.
(28) Lambooy, P.; Phelan, K. C.; Haugg, O.; Krausch, G. *Phys. Rev. Lett.* **1996**, *76*, 1110.
(29) Müller-Buschbaum, P.; Vanhoorne, P.; Scheumann, V.; Stamm, M. *Europhys. Lett.* **1997**, *40*, 655.
(30) Jacobs, K.; Herminghaus, S.; Mecke, K. R. *Langmuir* **1998**, *14*, 965.
(31) Jacobs, K.; Seemann, R.; Schatz, G.; Herminghaus, S. *Langmuir* **1998**, *14*, 4961.
(32) Sferrazza, M.; Heppenstall-Butler, M.; Cubitt, R.; Bucknall, D.; Webster, J.; Jones, R. A. L. *Phys. Rev. Lett.* **1998**, *81*, 5173.
(33) Xie, R.; Karim, A.; Douglas, J. F.; Han, C. C.; Weiss, R. A. *Phys. Rev. Lett.* **1998**, *81*, 1251.
(34) Müller-Buschbaum, P.; Gutmann, J. S.; Stamm, M. *Phys. Chem. Chem. Phys.* **1999**, *1*, 3857.
(35) Müller-Buschbaum, P.; Gutmann, J. S.; Stamm, M.; Cubitt, R.; Cunis, S.; von Krosigk, G.; Gehrke, R.; Petry, W. *Physica B* **2000**, *283*, 53.
(36) Götzelmann, A. Ph.D. Thesis, Mainz University, 1993.
(37) Schnell, R.; Stamm, M. *Physica B* **1997**, *234*−*236*, 247.
(38) Müller-Buschbaum, P.; O'Neill, S. A.; Affrossman, S.; Stamm, M. *Macromolecules* **1998**, *31*, 5003.
(39) Giessler, K. H.; Rauch, F.; Stamm, M. *Europhys. Lett.* **1994**, *27*, 605.
(40) Giessler, K.-H. Ph.D. Thesis, Frankfurt University, 1996.
(41) Giessler, K.-H.; Endisch, D.; Rauch, F.; Stamm, M. *Fresenius J. Anal. Chem.* **1993**, *346*, 151.
(42) Jung, W. G.; Fischer, E. W. *Macromol. Chem. Macromol. Symp.* **1988**, *16*, 281.
(43) Bartels, V. T.; Abetz, V.; Mortensen, K.; Stamm, M. *Europhys. Lett.* **1994**, *27*, 371.
(44) Gutmann, J. S.; Müller-Buschbaum, P.; Stamm, M. *Faraday Discuss.* **1999**, *112*, 285.
(45) Müller-Buschbaum, P.; Gutmann, J. S.; Stamm, M. *Macromolecules* **2000**, *33*, 4886.
(46) Parrat, L. G. *Phys. Rev.* **1954**, *55*, 359.
(47) Born, M.; Wolf, E. In *Principles of Optics*, 2nd ed.; Pergamon Press: Oxford, 1964.
(48) James, R. W. In *The Optical Principles of the Diffraction of X-Rays*; OxBow Press: Woodbridge, CT, 1962.
(49) Stamm, M.; Schubert, D. W. *Annu. Rev. Mater. Sci.* **1995**, *25*, 325.
(50) Gehrke, R. *Rev. Sci. Instrum.* **1992**, *63*, 455.
(51) Yoneda, Y. *Phys. Rev.* **1963**, *131*, 2010.
(52) Holý, V.; Baumbach, T. *Phys. Rev. B* **1994**, *49*, 10668.
(53) Müller-Buschbaum, P.; Gutmann, J. S.; Lorenz-Haas, C.; Mahltig, B.; Stamm, M.; Petry, W. *Macromolecules* **2001**, *34*, 7463.
(54) Limary, R.; Green, P. F. *Macromolecules* **1999**, *32*, 8167.
(55) Limary, R.; Green, P. F. *Langmuir* **1999**, *15*, 5617.
(56) Vrij, A.; Overbeek, J. T. G. *J. Am. Chem. Soc.* **1968**, *90*, 3074.
(57) Brochard, F.; Daillant, J. *Can. J. Phys.* **1990**, *68*, 1084.
(58) Vrij, A. *Faraday Discuss.* **1966**, *42*, 22.
(59) Brochard-Wyart, F.; Martin, P.; Redon, C. *Langmuir* **1993**, *9*, 3682.
(60) Fondecave, R.; Brochard-Wyart, F. *Macromolecules* **1998**, *31*, 9305.

MA010192Y